J. Biochem. 2011;150(6):607–614 doi:10.1093/jb/mvr097

JB THE JOURNAL OF BIOCHEMISTRY

Structure of *Thermus thermophilus* homoisocitrate dehydrogenase in complex with a designed inhibitor

Received June 14, 2011; accepted July 22, 2011; published online August 3, 2011

Eriko Nango[1,*], Takashi Yamamoto[1], Takashi Kumasaka[2] and Tadashi Eguchi[3,†]

[1]Department of Chemistry, Tokyo Institute of Technology, Tokyo Institute of Technology, O-okayama, Meguro-ku, Tokyo 152-8551; [2]Japan Synchrotron Radiation Research Institute, 1-1-1, Kouto, Sayo-cho, Sayo-gun, Hyogo 679-5198; and [3]Department of Chemistry and Materials Science, Tokyo Institute of Technology, O-okayama, Meguro-ku, Tokyo 152-8551, Japan

*Present address: Eriko Nango, RIKEN SPring-8 Center, SR Life Science Instrumentation Unit, 1-1-1, Kouto, Sayo-cho, Sayo-gun, Hyogo, 679-5148, Japan

†Tadashi Eguchi, Department of Chemistry and Materials Science, Tokyo Institute of Technology, O-okayama, Meguro-ku, Tokyo 152-8551, Japan. Tel/Fax: +81-3-5734-2631, email: eguchi@cms.titech.ac.jp

Homoisocitrate dehydrogenase (HICDH) is involved in the α-aminoadipate pathway of lysine biosynthesis in some bacteria and higher fungi, and catalyses the oxidative decarboxylation of (2*R*,3*S*)-homoisocitrate into 2-ketoadipate using NAD^+ as a coenzyme. In this study, the crystal structure of *Thermus thermophilus* HICDH in a binary complex with a designed inhibitor, (2*S*,3*S*)-thiahomoisocitrate, has been determined at 2.6 Å resolution. The inhibitor observed as a decarboxylated product interacts through hydrogen bonding to Arg 118, Tyr 125 and Lys 171 in the active site. The induced fitting was also observed around the region consisting of residues 120–141, which shifted up to 2.8 Å towards the active site. In addition, it was found that the complex structure adopts a closed conformation in two domains. While the structure of apo-HICDH shows that a catalytic residue Tyr 125 and Arg 85 that engages in substrate recognition are flipped out of the active site, these residues turn towards the active site in the complex structure. The results revealed that they directly interact with a substrate and are involved in catalysis or substrate recognition. Furthermore, by comparing the binary complex with the quaternary complex of *Escherichia coli* isocitrate dehydrogenase, the substrate recognition mechanism of HICDH is also discussed.

Keywords: α-aminoadipate pathway/crystal structure/homoisocitrate dehydrogenase/inhibitor/lysine biosynthesis.

Abbreviations: AIDS, acquired immune deficiency syndrome; NAD, nicotinamide adenine dinucleotide.

L-Lysine is an essential amino acid for human and animals, and is biosynthesized *de novo* in bacteria, lower eukaryotes and plants. Human pathogenic fungi such as *Candida albicans*, *Cryptococcus neoformans* and *Aspergillus fumigatus* represent a major health threat for patients with cancer, transplant patients and AIDS patients undergoing immunosuppressive treatment. These fungi as well as the plant pathogen *Magnaporthe grisea,* utilize the α-aminoadipate pathway for L-lysine biosynthesis (*1*). Since this pathway is unique for these organisms, enzymes involved in this pathway are considered to be a potential target for new anti-fungal drugs (*2*).

Homoisocitrate dehydrogenase (HICDH, EC 1.1.1.87) is involved in the α-aminoadipate pathway (*3*), and catalyses the conversion of homoisocitrate (HIC) to 2-ketoadipate through the oxidation of a hydroxyl group by nicotinamide adenine dinucleotide (NAD^+), subsequent decarboxylation and final protonation of the enolate as shown in Fig. 1. HICDH is a member of the family of β-hydroxy acid oxidative decarboxylases (*4*), which includes isocitrate dehydrogenase (ICDH), isopropylmalate dehydrogenase (IPMDH) and tartrate dehydrogenase. These enzymes recognize each 2*R*-substrate that differs in the C3 substituent and are similar in sequence, structure and catalytic mechanism.

HICDH is known to have different substrate specificity depending on species. For example, HICDHs from *Schizosaccharomyces pombe* and *Saccharomyces cerevisiae* utilize only HIC as a substrate (*5*, *6*). However, HICDH from *Deinococcus radiodurans* catalyses the oxidation of HIC, isocitrate and isopropylmalate (*7*). *Methanococcus jannaschii* HICDH accepts $(homo)_n$isocitrate ($n = 1$, 2 and 3), but recognizes neither isocitrate nor 3-isopropylmalate as a substrate (*8*). HICDH from *Thermus thermophilus* (TtHICDH) shows distinctive substrate specificity and can recognize isocitrate as a substrate at 20-fold higher efficiency than it does the native substrate, HIC (*5*).

The structures of HICDH have been reported only in wild (*9*) and its mutant (*10*) of apo-TtHICDH. The native structure showed that a catalytic residue Tyr 125 is flipped out of the active site. This tyrosine is conserved among β-hydroxy acid oxidative decarboxylases. In crystal structures of other β-hydroxy acid oxidative decarboxylases such as IPMDH from *Thiobacillus ferrooxidans* (*11*) and ICDH from *Escherichia coli* (EcICDH) (*12*), the tyrosine extends

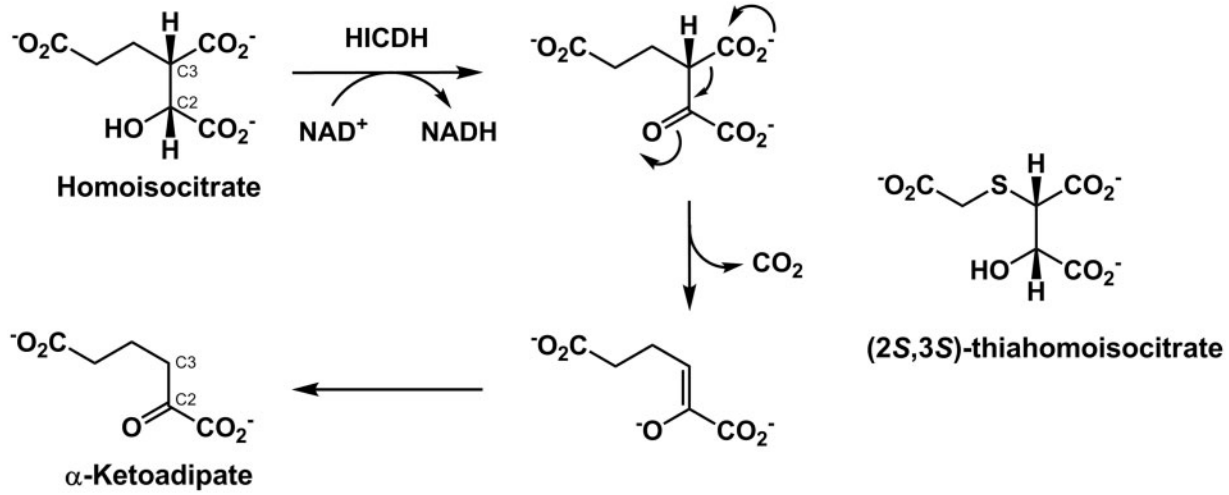

Fig. 1 Enzyme reaction of HICDH and structure of thiahomoisocitrate.

its side chain towards the substrate to function as the general acid that protonates the substrate after decarboxylation (*4*). In HICDH, it is considered that the tyrosine might interact with a substrate; however, its structural evidence has not been obtained so far even though a substrate, HIC or isocitrate was added to the crystallization solution (*9*). In addition, it is difficult to understand a reaction mechanism or substrate recognition of an enzyme from only the structure in the apo-from. There is thus an immediate need to clarify the structure of HICDH in complex with a substrate and/or a cofactor.

We have previously developed a racemic thiahomoisocitrate for HICDH from *S. cerevisiae* as a strong inhibitor (*13*). In this study, a chiral (2*S*,3*S*)-thiahomoisocitrate was synthesized for co-crystallization with HICDH, and the crystal structure of TtHICDH in a binary complex with this inhibitor was successfully determined at a resolution of 2.6 Å. In this structure, a decarboxylated product from the inhibitor was found to be tightly bound to residues in the active site of the structure. Furthermore, a conformational change in the loop of residues 121–128 was observed, and Tyr 125 extended its side chain towards the product. Also, we discuss the substrate recognition mechanism based on a comparison with the structure of ICDH in complex with a substrate and a cofactor.

Materials and Methods

Synthesis of (2S,3S)-(-)-thiahomoisocitrate

To a solution of (2*R*,3*R*)-epoxysuccinic acid (1.00 g, 7.57 mmol) in distilled water (25 ml) was added 3.0 M of aqueous sodium hydroxide until pH = 12. Then, thioglycolic acid (578 µl, 8.33 mmol) was added. The mixture was stirred for 10 h at 80°C. The solution was evaporated and the residue was chromatographed over ion-exchanged resin (DEAE Sephadex A-20, 0-3.0 M formic acid). Recrystallization by acetone-$CHCl_3$ gave (2*S*,3*S*)-(-)-thiahomoisocitrate (721 mg, 42%): IR (KBr): 3259, 1733, 1701 cm^{-1}; m.p. 155°C; ^{1}H NMR (D_2O) δ 4.47 (d, *J* = 5.1 Hz, 1H), 3.91 (d, *J* = 5.1 Hz, 1H), 3.45 (d, *J* = 16.4 Hz, 1H), 3.40 (d, *J* = 16.4 Hz, 1H); ^{13}C NMR (D_2O) δ 175.3, 174.7, 173.5, 72.0, 51.5, 34.4; *Anal.* Calcd for $C_6H_8O_7S$: C, 32.14; H, 3.60; S, 14.30, Found: C, 31.95; H, 3.78; S, 14.52, $[\alpha]_D^{23}$-53 (*c* = 1.0, H_2O).

Expression and purification

The HICDH gene was amplified by PCR from the genome of *T. thermophilus* HB8 with primers, thicdh-F (5′-GACATATGGCG TACCGGATCTGC-3′) and thicdh-R (5′-TGAATTCTACAGGCT CTTGAGCG-3′). PCR conditions: 1 cycle at 94°C for 5 min followed by 40 cycles of 94°C for 30 s, 55°C for 30 s and 68°C for 1 min using KOD-plus DNA polymerase (TaKaRa). The introduced NdeI site and EcoRI site are indicated by solid and dashed underlines, respectively. The amplified fragments were digested with EcoRV and EcoRI, and were cloned into LITMUS28 (New England Biolabs) to give LITMUS28-thicdh. After the nucleotide sequence was verified, the NdeI–EcoRI fragment of the resulting plasmid was subcloned into the corresponding site of pET30a (Novagen) to give pET-thicdh. The pET-thicdh was transformed into *E. coli* Rosetta (TaKaRa) for overexpression. TtHICDH was purified by the method described previously (*5*).

Inhibition assay

Kinetic measurements were performed at 60°C in an assay mixture (total 700 µl) containing 50 mM HEPES–NaOH (pH 7.8), 200 mM KCl, 5.0 mM $MgCl_2$, and 1.0 mM NAD^+. A reaction mixture including TtHICDH (10 µg/ml) and HIC (30–1000 µM) and the inhibitor was pre-incubated for ~5 min, and the reaction was started by addition of NAD^+ to the reaction mixture. The formation of NADH was measured at 340 nm for 20 s. The kinetic parameters were estimated by Hanes plots or Dixon plots.

Crystallization, data collection and molecular replacement

A solution of TtHICDH was concentrated to 60 mg/ml in 5 mM Tris–HCl at pH 7.8. Co-crystallization of TtHICDH with the thiahomoisocitrate and NAD^+ was performed by vapour diffusion using sitting drops of the crystallization solution at 20°C. A 2 µl droplet of 9.8 mg/ml protein solution containing 0.8 mM of the inhibitor and 1.7 mM NAD^+ mixed with the same amount of reservoir solution was equilibrated against 1 ml reservoir solution (40% MPD and 100 mM citrate pH 4.85). Square plate-shaped crystals were obtained in 2 weeks. Prior to data collection, crystals were transferred to fresh drops containing reservoir solution supplemented with 0.5 mM inhibitor, 0.5 mM NAD^+ and 42% (v/v) MPD and flash-cryocooled by transfer directly into a cold stream of nitrogen gas (100 K). Diffraction data were collected on a Jupiter 210 CCD detector at beamline BL26B1 (SPring-8, Japan) (*14*) using a mail-in data collection system with the approval of RIKEN (Proposal No. 20080020). Data were processed with the *HKL*-2000 processing suite (*15*). The resulting crystal belongs to space group *C*2 (*a* = 221.0 Å, *b* = 93.70 Å, *c* = 88.80 Å and β = 97.68 Å). The asymmetric unit contains four protein molecules and 61% solvent. The crystallographic statistics are given in Table I. The complex structure was solved by molecular replacement using MOLREP (*16*) with the TtHICDH structure (PDB entry 1X0L) as a search model. Model building and refinement

Table I. Summary of crystallographic statistics.

	TtHICDH complex
Data collection	
Wavelength (Å)	1.00
Resolution range (Å)	44.0–2.60
Observed reflections	270 793
Unique reflections	55 139
I/σ (I)	5.7 (2.5)
R_{merge} (%)[a]	11.5 (40.6)
Data completeness (%)	99.8 (99.3)
Redundancy	3.6 (3.2)
Refinement	
Resolution range (Å)	44.0–2.60
R_{work} (%), (number of reflections)	16.9 (52 340)
R_{free} (%), (number of reflections)	23.1 (2799)
R.m.s.d. bond length (Å)/angle (°)	0.014/1.57
Average B factors (Å^2)	33.5
Main chain	32.6
Side chain	34.3
Solvent	33.4
Ligands	33.5

Values in parentheses are for the highest resolution shell.
[a]$R_{merge} = \Sigma_{hkl}\ \Sigma_i\ |\ I_i(hkl) - <I(hkl)>|\ /\ \Sigma_{hkl}\Sigma_i\ I_i(hkl)$, where $I_i(hkl)$ is the ith intensity measurement of reflection hkl, including symmetry-related reflections, and $<I(hkl)>$ is its average.

were carried out with Coot (*17*) and REFMAC5 (*18*). The final models were refined to 2.60 Å with R_{work} and R_{free} values of 0.169 and 0.231, respectively. The final refinement statistics are given in Table I. Molecular graphic figures were created using PyMOL (*19*). The coordinates have been deposited in the Protein Data Bank (3ASJ).

Results

Inhibitor activity and structural changes by inhibitor binding

The chiral thiahomoisocitrate was synthesized according to the previously reported method (*13*) using (2*R*,3*R*)-epoxysuccinic acid as a starting material. The synthesized (2*S*,3*S*)-thiahomoisocitrate was subjected to reaction with TtHICDH. The reactions were monitored by measuring the formation of NADH from NAD^+. As a result, this compound appeared to act as a competitive inhibitor ($K_i = 13\ \mu M$). Comparing this result with the K_m value for HIC (7.5 mM) (*5*), (2*S*,3*S*)-thiahomoisocitrate was shown to have a strong inhibitory activity against TtHICDH.

We next carried out co-crystallization screening with the enzyme, the inhibitor and NAD^+ and obtained crystals suitable for X-ray analysis. The X-ray structure of the binary complex was solved by molecular replacement phasing against data to 2.60 Å. The overall structure of the complex is shown in Fig. 2A. The overall tetramer assembly is almost same with the reported native structure (*9*); however, the inhibitors was observed as a decarboxylated product in each active site of three subunits, and the significant conformational change caused by binding to the inhibitor was found.

Superimposition of the native and the complex structure of TtHICDH is shown in Fig. 2B. One difference is related to the open–close movement in the two domains, that is, the complex structure adopts a closed conformation, which is similar to the closed conformation of the structure of IPMDH from *T. ferrooxidans* in complex with a substrate (*11*). The other is the induced fitting around a loop-containing region composed of residues 120–141, which shifted up to 2.8 Å towards the active site. The catalytic residue, Tyr 125, on the loop (residues 121–128) forms a hydrogen bond to the carboxymethylthio group of the product in the active site, while the residue is flipped out of the substrate binding site in the structure of apo-TtHICDH. Comparing the Ramachandran plot of the apo-TtHICDH structure and the complex structure, the backbone torsion angles (the ϕ and ψ angles) of Glu 122, Gly 123, Tyr 125, Val 126 and Glu 127 vary considerably. In particular, the ϕ, ψ angles of Gly 123 change from the allowed region for non-glycine residues in the Ramachandran plot ($\phi = 72.4°$, $\psi = 24.5°$) to the forbidden region for non-glycine residues ($\phi = 66.0°$, $\psi = -137.8°$) in response to ligand binding. The results indicate that Gly 123 might play a significant role during the conformational change.

Active site structure

The decarboxylated product resulting from the inhibitor is located in the cleft between two domains as shown in Fig. 2C. This indicates that the oxidation of the inhibitor by NAD^+ proceeds and the inhibition is caused by a slow reaction after the decarboxylation. Each inhibitor showed a similar conformation. Most products from the inhibitor existed in the form of enol/enolate rather than the keto form although the product in only subunit A seemed to exist in both the enol/enolate form and the keto form. However, the conformations of the residues in the active site cleft, Arg 85, Arg 88, Asn 96, Arg 98, Arg 118, Tyr 125, Lys 171′, Asp 204', Asp 228 and Asp 232 (the primes indicate a neighbour subunit), were similar across the subunits. The product forms a hydrogen bond with the side chains of Arg 85, Arg 88, Arg 118, Tyr 125 and Lys 171′. In particular, Tyr 125 and Lys 171′ are tightly bound to the carboxymethylthio group of the product. Arg 118 binds through a hydrogen bond to the hydroxyl group of the product, and Arg 98 interacts with the C2 carboxylate group of the product. Only Arg 85 in subunit D, which forms a hydrogen bond to Glu 127, shows the different conformation with others, turning outside of the active site.

In the structure of apo-TtHICDH, the side chains of Arg 85 and Tyr 125 are directed away from the active site even though it has been suggested that Arg 85 is involved in the recognition of the substrate and that Tyr 125 functions as a catalytic residue (*5*, *9*). In the complex structure, these residues interact with the product which is similar to an original product, α-ketoadipate, indicating that they are involved in the enzyme reaction.

NAD^+ binding

Although NAD^+ and an essential magnesium ion were added to the crystallization solution, they were not found anywhere. Recently, we have reported the crystal structure of IPMDH from *T. thermophilus* (TtIPMDH) in a ternary complex with NAD^+ and a designed inhibitor, (2*S*,3*S*)-(-)-3-methylmercaptomalic acid which is a sulphur substituted substrate analog as

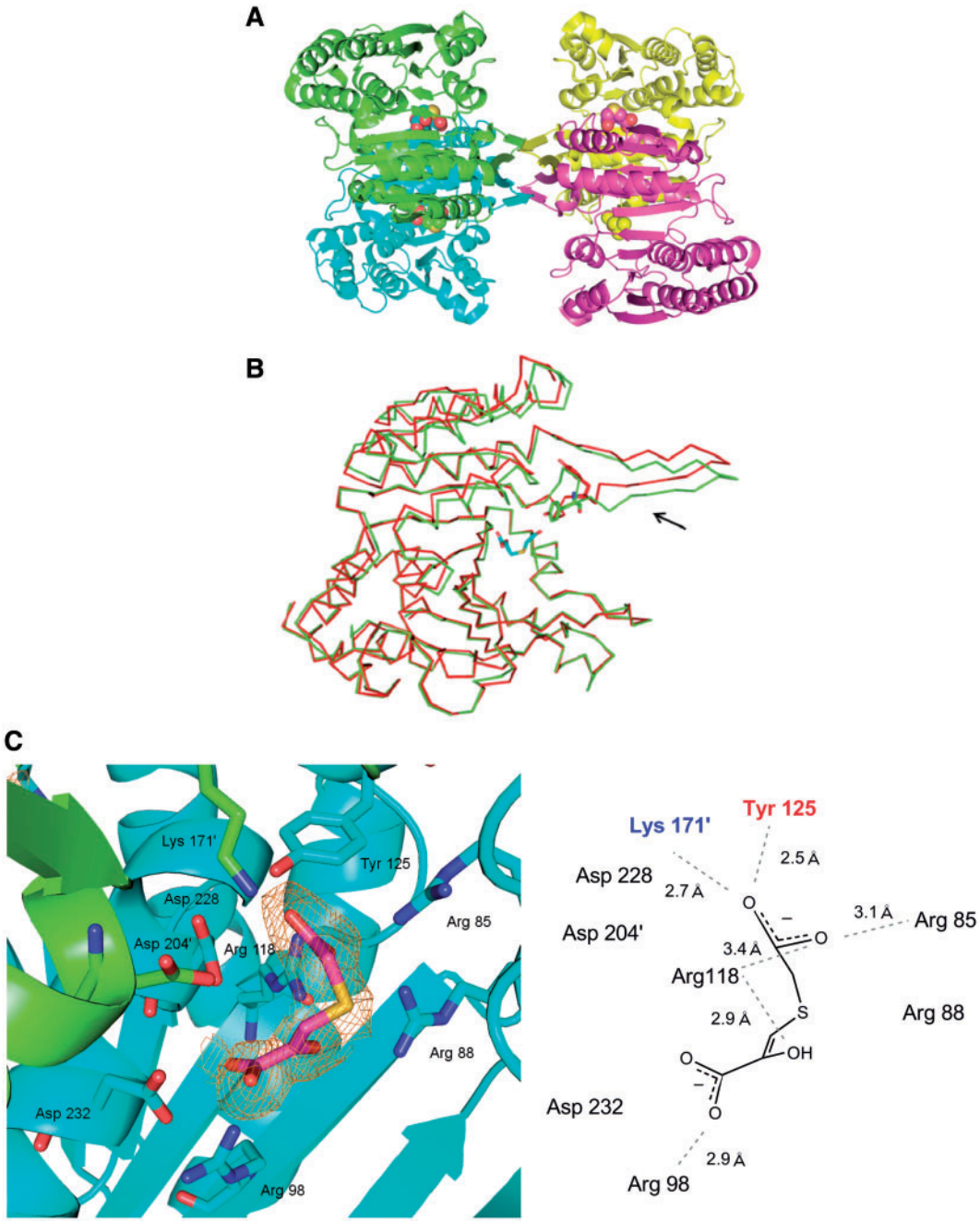

Fig. 2 Structure of the TtHICDH–inhibitor complex. (A) Schematic drawing of the tetramer of the complex. (B) Superimposition of the TtHICDH binary complex (green) onto the apo-TtHICDH structure (red, PDB entry 1X0L). The region indicated by the arrow is the loop between Thr 120 and Val 141. Tyr 125 is drawn as a stick. (C) Omit map covering the inhibitor in the active site of subunit B (contour level 2σ) and schematic drawing of the product-binding site.

well as thiahomoisocitrate (*20*). The inhibitor also existed as a decarboxylated product in the ternary structure of TtIPMDH. However, NAD^+ was definitely present in this structure. Similarly, complex structures of ICDH derived from various species showed a cofactor ($NADP^+$ or NAD^+) tightly bound to the enzyme (*20–22*). Thus, it seems that TtHICDH binds weakly to cofactors compared with other β-hydroxy acid oxidative decarboxylases although K_m for NAD^+ was not determined using HIC as substrate, and there is a possibility that the metal or the cofactor might remain in the active site if crystals can be obtained under higher pH condition.

Given the amino acid sequence alignment of HICDHs and IPMDHs from various sources, amino acid residues that interact with the adenine-ribose portion of NAD^+ in TtIPMDH (*23*) are all conserved between HICDHs. However, TtHICDH lacks a residue corresponding to Asp 78 that interacts with the nicotinamide ribose moiety of NAD^+ in TtIPMDH. Ile 84 in TtHICDH corresponds to Glu 87 bound to the nicotinamide ribose moiety of NAD^+ in

TtIPMDH. Therefore, TtHICDH might have a weaker affinity for NAD^+ than TtIPMDH.

Discussion

Inhibition mechanism by thiahomoisocitrate

We previously proposed the inhibitory mechanism of thiahomoisocitrate as follows (*13*): once the thia-substrate analogue is accepted by HICDH, the enzyme reaction proceeds partially. The stability of the intermediary enolate (or enol) is increased by sulphur substitution, and the enolate intermediate might reside within the active site due to the slow tautomerization step. As we expected, the complex structure shows that the decarboxylated product resides in the active site, which reveals that the inhibition is caused by the slow reaction after decarboxylation. Because most of inhibitors in the crystal structure are observed in the form of enol/enolate, it seems that the stable enol/enolate product is predominantly involved in the inhibition.

Actually, the product exists in the enol/enolate form rather than the keto form in the structure of TtIPMDH in complex with the thia-analogue inhibitor, and all the observed interactions between the product and residues in the active site are likely to be involved in the keto–enol tautomerization (*20*).

On the other hand, in the complex structure of TtHICDH, the enzyme interacts not only with the hydroxyl group of the enol/enolate product, but also with the two carboxylic groups of the product. In particular, the strong interaction of the carboxymethylthio group of the product with Tyr 125 and Lys 171′ was observed. These hydrogen-bonding interactions would prevent the product from being released at the active site of TtHICDH. Thus, the complex structure suggests that multiple factors such as the effect of the stable enol/enolate and the hydrogen bonding between two carboxylic groups of the product and residues are engaged in the inhibitory mechanism (Fig. 3).

Implication for substrate recognition mechanism

ICDH is very similar to HICDH in amino acid sequence and substrate among the family of β-hydroxy acid oxidative decarboxylases. Many complex structures of ICDH containing the structure in complex with both a cofactor and a substrate were reported. Thus, we compared the binary complex of TtHICDH to the quaternary complex of ICDH from EcICDH (*12*).

The superimposition of the active site of the binary complex of TtHICDH on that of the quaternary complex of EcICDH shows that both active sites are quite similar (Fig. 4A). The residues interacting with isocitrate in EcICDH are well conserved also in TtHICDH except for Ser 113 and Asn 115 in EcICDH, which recognizes the carboxymethyl group of isocitrate. Ser 113 corresponds to Gly 82 in TtHICDH based on amino acid sequence alignments, and Asn 115 corresponds to Ile 84 in TtHICDH, which is highly conserved among HICDHs from various species. However, the side chain of Arg 85 in TtHICDH is located at the position of Ser 113 in EcICDH. Previous mutation analysis has indicated that Arg 85 is one of the most important residues for substrate recognition in TtHICDH (*5*). Arg 85 should participate in the recognition of the carboxyethyl group of HIC as the corresponding residue to Ser 113 in EcICDH.

The substrate recognition mechanism of TtHICDH is suggested as shown in Fig. 4B. Previously, the results of mutational studies have suggested that Tyr 125 and Lys 171′ function as a general acid—general base pair (*9*, *24*). In fact, these residues are bound to the product strongly and seem to prevent the product from being released at the active site. Tyr 125 is likely to interact with the C3 carboxylate of HIC in the HICDH reaction, and Lys 171′ may be bound to the hydroxyl group of HIC.

As described above, HICDH is known to show different substrate specificity depending on species. TtHICDH has a broad specificity for the C3 side chain of the substrate (*5*). Indeed, it recognizes isocitrate as a substrate, in contrast to HICDHs from *S. pombe* and *S. cerevisiae* which predominantly recognize HIC (*6*). Intriguingly, there is no residue that is involved in the recognition of the carboxyethyl group of HIC except Arg 85. Structural studies for IPMDH and ICDH have revealed that amino acid residues in a loop between β-strand 3 and α-helix 4 are involved in the substrate specificity of the enzymes of the β-hydroxy acid oxidative decarboxylase family (*13*, *25*, *26*). In case of TtHICDH, Arg 85 is located in a loop between β-strand 3 and α-helix 4. The amino acid residues in the loop between β-strand 3 and α-helix 4 are quite different between TtHICDH and *S. cerevisiae* HICDH (ScHICDH). A mutation of TtHICDH, which is altered into the same sequence as that of ScHICDH in the loop, induced change of the substrate specificity and the mutant recognized HIC rather than isocitrate (*5*). In the complex of TtHICDH, most of the loop region (from Pro 78 to Tyr 86) is located outside the active site, and only Arg 85 participates in the active site, which causes a relatively wide space in the

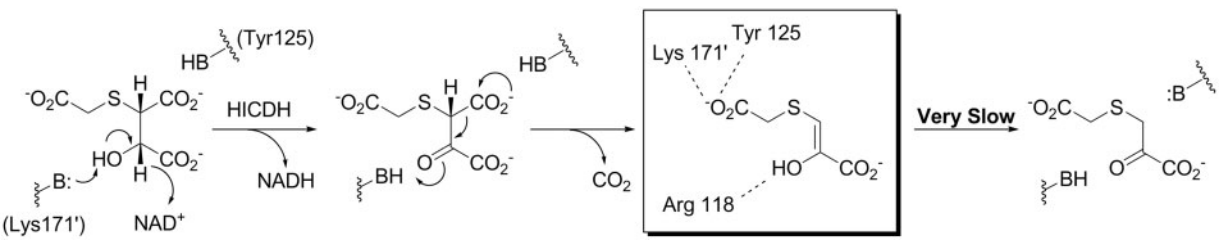

Fig. 3 Inhibition mechanism of thiahomoisocitrate against HICDH.

vicinity of the carboxyethyl group of the substrate in TtHICDH. These factors could cause the broad specificity of TtHICDH.

In addition, HICDH from *D. radiodurans* (DrHICDH) also has broad substrate recognition (*7*, *27*). The residues in the active site are highly conserved between TtHICDH and DrHICDH. Comparing these enzymes (group A) with HICDHs that have a high substrate specificity such as *S. pombe* or *S. cerevisiae* HICDH (group B), the amino acid residues responsible for the recognition of the malate moiety are conserved, but the residues involved in the recognition of the C3 side chain of the substrate (the loop between β-strand 3 and α-helix 4) are different. The region that differs between groups A and B is shown in Fig. 5.

The amino acid residues corresponding to Ser 113 and Val 116 in EcICDH are conserved in group B. The isoleucine residue corresponding to Asn 115 (EcICDH) is conserved in both groups. Therefore, the isoleucine residue (Ile 87 in TtHICDH) may play an important role in HICDH reactions such as interaction with the ethylene chain of HIC. In fact, the isoleucine residue is located in the active site in the complex structure. Interestingly, the valine residue conserved in group B is replaced by an arginine residue in group A. In the complex structure, Arg 85, corresponding to Val 116 in EcICDH, appears to participate in the recognition of the carboxyethyl group of HIC. Thus, the substitution of the arginine residue would affect the substrate specificity for HICDH of group A. Although no other structure has been reported except for TtHICDH, the serine residue corresponding to Ser 113 in EcICDH may take part in the recognition of the carboxyethyl group of HIC in group B because the overall structures of group B are expected to be similar to those of TtHICDH and EcICDH.

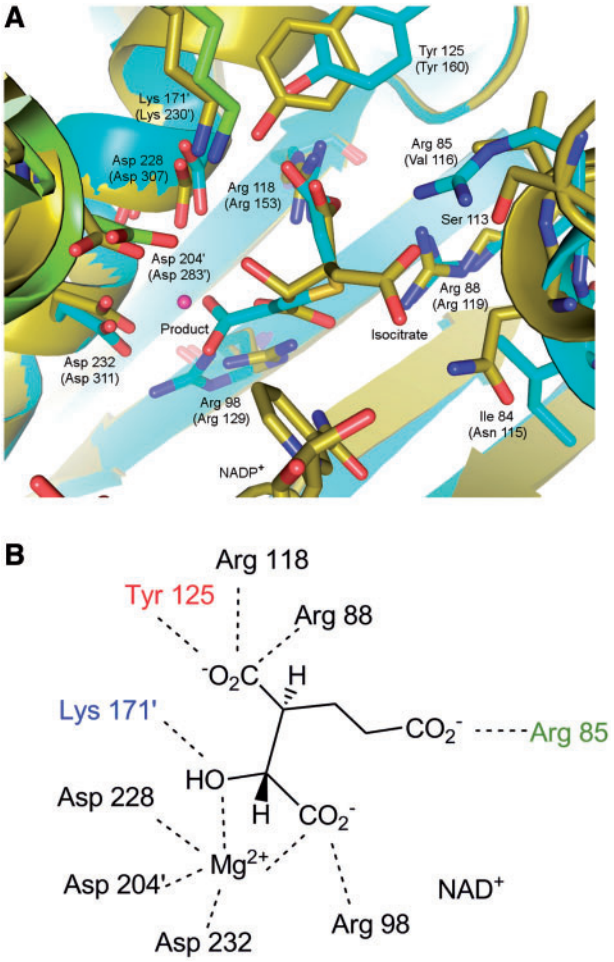

Fig. 4 Proposed substrate recognition mechanism. (A) Superimposition of the TtHICDH binary complex active site residues (cyan and green) onto the quaternary complex of EcICDH residues (yellow, PDB entry 1AI2). Calcium ion (pink) is coordinated to isocitrate. The corresponding residues for the EcICDH complex are shown in parentheses. (B) Schematic drawing of proposed recognition mechanism.

Conclusions

The synthesized (2*S*,3*S*)-(-)-thiahomoisocitrate showed a strong competitive inhibitory activity towards TtHICDH. We determined the crystal structure of TtHICDH in complex with the inhibitor as the first example of a complex structure of HICDH. The structure showed a decarboxylated product in the active site and the strong interaction of the product with the residues, Tyr 125 and Lys 171′, in the active site. These results indicate that the tautomerization step of the inhibitor during the HICDH reaction is involved in the inhibition. In addition, the structure showed a fully closed conformation, where the region consisting of residues 120–141 changed its structure significantly compared with apo-TtHICDH. In particular, Tyr

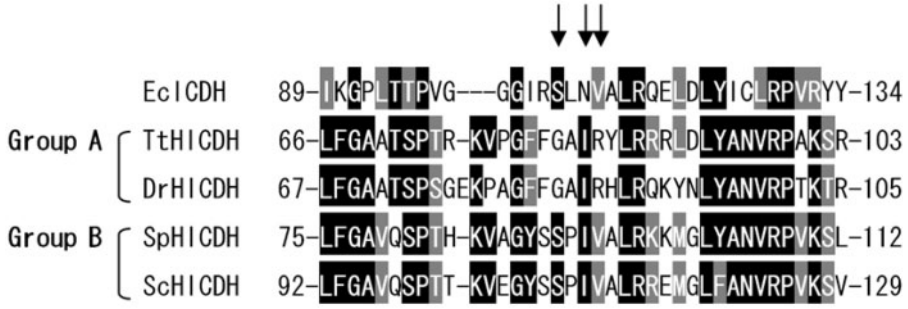

Fig. 5 Multiple alignment of the amino acid sequences containing the loop between β-strand 3 and α-helix 4 in EcICDH and HICDHs from various species. EcICDH, ICDH from *E. coli*; SpHICDH, HICDH from *S. pombe*; ScHICDH, HICDH from *S. cerevisiae*; TtHICDH, HICDH from *T. thermophilus*; DrHICDH, HICDH from *D. radiodurans*.Ser 113, Asn 115 and Val 116 in EcICDH are indicated by arrows.

125 takes part in the active site while the residue is directed away from the active site in the apo form.

Further, the substrate recognition mechanism of TtHICDH was proposed based on a structural comparison with the quaternary complex of EcICDH. Given the structural similarity, only Arg 85 would be involved in the recognition of the C3 side chain of the substrate, and a relatively wide space appears to exist in the vicinity of the carboxyethyl group of the substrate. This space may cause the broad specificity of TtHICDH.

Since HICDH is involved in the α-aminoadipate pathway for L-lysine biosynthesis that is specific to human and plant pathogenic fungi, our discovery of the structure of a binary complex of TtHICDH should be useful for the structure-assisted design of antifungal agents as well as elucidation of enzyme reaction mechanisms.

Acknowledgements

The authors thank Dr Masaki Yamamoto for the collection of data at SPring-8 BL26B1 via the mail-in data collection system.

Conflict of interest
None declared.

References

1. Zabriske, M. and Jackson, M. (2000) Lysine biosynthesis and metabolism in fungi. *Nat. Prod. Rep.* **17**, 85–97
2. Palmer, D.R., Balogh, H., Ma, G., Zhou, X., Marko, M., and Kaminskyj, S.G. (2004) Synthesis and antifungal properties of compounds which target the alpha-aminoadipate pathway. *Pharmazie* **59**, 93–98
3. Strassman, M. and Ceci, L.N. (1965) Enzymatic formation of alpha-ketoadipic acid from homoisocitric acid. *J. Biol. Chem.* **240**, 4357–4361
4. Aktas, D.F. and Cook, P.F. (2009) A lysine-tyrosine pair carries out acid-base chemistry in the metal ion-dependent pyridine dinucleotide-linked beta-hydroxyacid oxidative decarboxylases. *Biochemistry* **48**, 3565–3577
5. Miyazaki, J., Kobashi, N., Nishiyama, M., and Yamane, H. (2003) Characterization of homoisocitrate dehydrogenase involved in lysine biosynthesis of an extremely thermophilic bacterium, *Thermus thermophilus* HB27, and evolutionary implication of beta-decarboxylating dehydrogenase. *J. Biol. Chem.* **278**, 1864–1871
6. Chen, R. and Jeong, S.S. (2000) Functional prediction: identification of protein orthologs and paralogs. *Protein Sci.* **9**, 2344–2353
7. Miyazaki, K. (2005) Identification of a novel trifunctional homoisocitrate dehydrogenase and modulation of the broad substrate specificity through site-directed mutagenesis. *Biochem. Biophys. Res. Commun.* **336**, 596–602
8. Howell, D.M., Graupner, M., Xu, H., and White, R.H. (2000) Identification of enzymes homologous to isocitrate dehydrogenase that are involved in coenzyme B and leucine biosynthesis in methanoarchaea. *J. Bacteriol.* **182**, 5013–5016
9. Miyazaki, J., Asada, K., Fushinobu, S., Kuzuyama, T., and Nishiyama, M. (2005) Crystal structure of tetrameric homoisocitrate dehydrogenase from an extreme thermophile, *Thermus thermophilus*: involvement of hydrophobic dimer-dimer interaction in extremely high thermotolerance. *J. Bacteriol.* **187**, 6779–6788
10. Suzuki, Y., Asada, K., Miyazaki, J., Tomita, T., Kuzuyama, T., and Nishiyama, M. (2010) Enhancement of the latent 3-isopropylmalate dehydrogenase activity of promiscuous homoisocitrate dehydrogenase by directed evolution. *Biochem. J.* **431**, 401–410
11. Imada, K., Inagaki, K., Matsunami, H., Kawaguchi, H., Tanaka, H., Tanaka, N., and Namba, K. (1998) Structure of 3-isopropylmalate dehydrogenase in complex with 3-isopropylmalate at 2.0 A resolution: the role of Glu88 in the unique substrate-recognition mechanism. *Structure* **6**, 971–982
12. Mesecar, A.D., Stoddard, B.L., and Koshland, D.E. Jr (1997) Orbital steering in the catalytic power of enzymes: small structural changes with large catalytic consequences. *Science* **277**, 202–206
13. Yamamoto, T. and Eguchi, T. (2008) Thiahomoisocitrate: a highly potent inhibitor of homoisocitrate dehydrogenase involved in the alpha-aminoadipate pathway. *Bioorg. Med. Chem.* **16**, 3372–3376
14. Ueno, G., Kanda, K., Hirose, R., Ida, K., Kumasaka, T., and Yamamoto, M. (2006) RIKEN structural genomics beamlines at the SPring-8; high throughput protein crystallography with automated beamline operation. *J. Struct. Funct. Genomics* **7**, 15–22
15. Otwinowski, Z. and Minor, W. (1997) Processing of X-ray diffraction data collected in oscillation mode. *Methods Enzymol.* **276**, 307–326
16. Vagin, A. and Teplyakov, A. (2010) Molecular replacement with MOLREP. *Acta Crystallogr. D Biol. Crystallogr.* **66**, 22–25
17. Emsley, P. and Cowtan, K. (2004) Coot: model-building tools for molecular graphics. *Acta Crystallogr. D Biol. Crystallogr.* **60**, 2126–2132
18. Murshudov, G.N., Vagin, A.A., Lebedev, A., Wilson, K.S., and Dodson, E.J. (1999) Efficient anisotropic refinement of macromolecular structures using FFT. *Acta Crystallogr. D* **55**, 247–255
19. DeLano, W.L. (2002) *The PYMOL Molecular Graphic System.*, DeLano Scientific LLC, San Carlos, CA, USA
20. Nango, E., Yamamoto, T., Kumasaka, T., and Eguchi, T. (2009) Crystal structure of 3-isopropylmalate dehydrogenase in complex with NAD(+) and a designed inhibitor. *Bioorg. Med. Chem.* **17**, 7789–7794
21. Xu, X., Zhao, J., Xu, Z., Peng, B., Huang, Q., Arnold, E., and Ding, J. (2004) Structures of human cytosolic NADP-dependent isocitrate dehydrogenase reveal a novel self-regulatory mechanism of activity. *J. Biol. Chem.* **279**, 33946–33957
22. Peng, Y., Zhong, C., Huang, W., and Ding, J. (2008) Structural studies of *Saccharomyces cerevesiae* mitochondrial NADP-dependent isocitrate dehydrogenase in different enzymatic states reveal substantial conformational changes during the catalytic reaction. *Protein Sci.* **17**, 1542–1554
23. Hurley, J.H. and Dean, A.M. (1994) Structure of 3-isopropylmalate dehydrogenase in complex with NAD+: ligand-induced loop closing and mechanism for cofactor specificity. *Structure* **2**, 1007–1016
24. Lin, Y., West, A.H., and Cook, P.F. (2009) Site-directed mutagenesis as a probe of the acid-base catalytic mechanism of homoisocitrate dehydrogenase from *Saccharomyces cerevisiae*. *Biochemistry* **48**, 7305–7312

25. Imada, K., Sato, M., Tanaka, N., Katsube, Y., Matsuura, Y., and Oshima, T. (1991) Three-dimensional structure of a highly thermostable enzyme, 3-isopropylmalate dehydrogenase of *Thermus thermophilus* at 2.2 A resolution. *J. Mol. Biol.* **222**, 725–738
26. Hurley, J.H., Thorsness, P.E., Ramalingam, V., Helmers, N.H., Koshland, D.E. Jr, and Stroud, R.M. (1989) Structure of a bacterial enzyme regulated by phosphorylation, isocitrate dehydrogenase. *Proc. Natl. Acad. Sci. USA* **86**, 8635–8639
27. Yamamoto, T., Miyazaki, K., and Eguchi, T. (2007) Substrate specificity analysis and inhibitor design of homoisocitrate dehydrogenase. *Bioorg. Med. Chem.* **15**, 1346–1355